*Chinese Journal of*
**POLYMER SCIENCE**

RESEARCH ARTICLE

https://doi.org/10.1007/s10118-023-2992-5
*Chinese J. Polym. Sci.* **2023**, *41*, 1846–1855

# Stabilize and Reinforce Hydrogen-Bonded Polymer Complex Elastic Fiber by Catechol Chemistry and Coordination

Ze-Xin Liu†, De-Zhong Liu†, Cai-Hong Zhang, Wei-Jie Wang, Hao Huang, and Shu-Guang Yang*

*State Key Laboratory for Modification of Chemical Fibers and Polymer Materials, Center for Advanced Low-Dimension Materials, College of Materials Science and Engineering, Donghua University, Shanghai 201620, China*

Electronic Supplementary Information

**Abstract** Hydrogen-bonded polymer complex fiber of poly(ethylene oxide) (PEO) and poly(acrylic acid) (PAA) shows rubber elasticity in ambient environment, but the fiber has relatively low strength and weak stability. We apply the catechol chemistry and metal coordination to stabilize and strengthen the PEO/PAA fiber. PAA is grafted with dopamine (Dopa), and then combines with PEO to prepare fiber. PAA-Dopa in the fiber is cross-linked through oxidation induced dismutation and the metal ions are introduced through coordination. The cross-linking and coordination greatly improve the stability of the fiber against the erosion of alkaline water. Among four different metal coordination fibers, PEO/PAA-Dopa/Cu fiber keeps the excellent extensibility (~1000%) and presents much higher initial modulus (~7 MPa), ultimate strength (~20 MPa), and toughness (~60 MJ/m$^3$) than its precursor PEO/PAA fiber. In addition, PEO/PAA-Dopa/Cu fiber shows quick recovery and large energy dissipation ratio compared with the PEO/PAA fiber. The distinct mechanical properties enhancement of the hydrogen-bonded complex fiber is attributed to the synergy of hydrogen bonds, coordination and covalent bond cross-linking.

**Keywords** Elastic fiber; Hydrogen-bonded complexation; Catechol chemistry; Coordination; Elastomer

**Citation:** Liu, Z. X.; Liu, D. Z.; Zhang, C. H.; Wang, W. J.; Huang, H.; Yang, S. G. Stabilize and reinforce hydrogen-bonded polymer complex elastic fiber by catechol chemistry and coordination. *Chinese J. Polym. Sci.* **2023**, *41*, 1846–1855.

## INTRODUCTION

Elastomers are used as tires, seals, dampers, gloves, and special clothes, and are essential materials for modern technologies and our daily life.[1–7] The structure requirements of elastomers include the flexible and amorphous segments which save large entropy and cross-linkages which resist the permanent flow and creep.[8,9] Elastomers are cross-linked by covalent bonds or secondary interaction such as glass domains, crystallization domains, ionic aggregates, and hydrogen bonding complexes.[10–19]

Shaping elastomers into fibers greatly broaden their application territory.[20–29] The fiber of natural rubber was realized with intricate emulsion spinning.[24,25] Polyolefin and polyester-ether based elastic fibers are industrialized with small scale.[5,26,27] The most commercially successful elastic fiber is polyurethane Spandex fiber.[20,28,29] Hydrogen-bonded polymer complex elastic fiber not only show the mechanical properties similar with traditional elastomer materials but also exhibit special dynamic properties, such as self-healing, shape-memory, and stimuli-response.[30–33] Our group reported a highly elastic fiber from hydrogen-bonded polymer complex of poly(ethylene oxide) (PEO) and poly(acrylic acid) (PAA).[30] The hydrogen bonding complexation is restricted first to obtain spinnable fluid, and in the coagulation bath the reconstruction of interchain hydrogen bonding make the fiber formation. Hydrogen-bonded PEO/PAA fiber shows high extensibility and good recovery. However, the modulus, strength, and toughness of PEO/PAA fiber are relatively low, and PEO/PAA fiber is not stable at high pH value. Therefore, hydrogen-bonded PEO/PAA fiber needs to be stabilized, strengthened, and toughened for further application exploration.

Adding fillers, such as carbon black or fine silica particles, are widely used in industry to strengthen rubber materials.[34,35] Interpenetrating network, such as double network and triple network, are dedicated designed to produce tough elastic materials.[10,13,36–42] The reversible and sacrificial bonds, including metal coordination, hydrogen bonding, and electrostatic interaction, are intentionally combined with the basic covalent network to enhance toughness.[12–15,43,44] The covalent cross-linkages bridge the micro-cracks and maintain the intact of the whole system while the breakage of non-covalent interactions adsorbs and dissipates the energy, which greatly improving the toughness.[45,46]

Catechol and its derivatives present various chemical reactions and secondary interaction modes, and have intensively studied and utilized for functional materials design and pre-

* Corresponding author, E-mail: shgyang@dhu.edu.cn
† These authors contributed equally to this work.
Received March 1, 2023; Accepted April 17, 2023; Published online June 12, 2023

paration.[47–52] For example, Filippidi *et al*. applied mussel inspired iron-catechol complexes to tough epoxy-based elastomer.[50] They prepared loosely cross-linked amorphous epoxy network with ~14 mol% catechol content and subsequently treated with iron to form dynamic iron-catechol cross-links, resulting in modulus 184 MPa and keeps the elongation strain 150%.

In this work, we graft dopamine (Dopa) to PAA. PAA-Dopa is combined with PEO to prepared hydrogen-bonded polymer complex fiber. The pristine PEO/PAA-Dopa fibers are oxidized by $NaIO_4$ to form covalent bonds between PAA-Dopa, which increases the stability of the fiber. The covalent cross-linked fibers are further immersed into the metal salt solution to introduce coordination. Four kinds of metal ions, $Al^{3+}$, $Fe^{3+}$, $Zn^{2+}$ and $Cu^{2+}$, have been successfully incorporated into the fiber separately, and hence the stiffness of the fiber is greatly improved. Among these four fibers, PEO/PAA-Dopa/Cu fiber keeps excellent extensibility like its precursor PEO/PAA fiber, while shows much higher strength and toughness. The synergy of hydrogen bonding, coordination, and covalent cross-linking make the fibers have featured mechanical properties, rubber elasticity, self-healing and environmental adaptivity. The work will enlighten us to design and prepare the high-performance elastomer with dedicated combination and synergy of various secondary interactions and covalent bond cross-linking.

## EXPERIMENTAL

### Materials

Poly(acrylic acid) (PAA, $M_w$~$4.5\times10^5$ g·mol$^{-1}$), poly(ethylene oxide) (PEO, $M_w$~$6\times10^5$ g·mol$^{-1}$), dopamine hydrochloride (Dopa, >98%), 1-ethyl-3(3-(dimethylamino)propyl) carbodiimide (EDC, >98%), and sodium periodate ($NaIO_4$, AR) were purchased from Sigma-Aldrich. Sodium hydroxide (NaOH, AR), hydrochloric acid (HCl, AR), copper chloride dihydrate ($CuCl_2{\cdot}2H_2O$, AR), ferric chloride ($FeCl_3$, AR), aluminum chloride ($AlCl_3$, AR), zinc chloride ($ZnCl_2$, AR), sodium dihydrogen phosphate dihydrate ($NaH_2PO_4{\cdot}2H_2O$, AR), and disodium hydrogen phosphate dodecahydrate ($Na_2HPO_4{\cdot}12H_2O$, AR) were obtained from Shanghai Lingfeng Chemical Reagent. All chemicals were used as received without further purification. Dopa was linked as side group of PAA, and the product was marked as PAA-Dopa. The graft degree was mainly controlled at 5%. The synthesis and characterization of PAA-Dopa was described in the electronic supplementary information (Scheme S1 and Figs. S1–S3 in ESI).

### PEO/PAA Fibers Preparation

PEO/PAA fibers were prepared by the method similar to wet-spinning. Briefly, PAA solution and PEO solution were mixed with presence of hydroxide solution at a molar ratio of 1:1 (accounted with repeating unit) to obtain homogenous spinning solution (concentration 6.5 wt%). After removal of air bubbles, the solution was extruded through a 0.21 mm spinneret (single hole) into a 2.0 mol/L HCl coagulation bath to obtain fiber. The PEO/PAA fibers were spontaneously dried in ambient environment. The diameter of PEO/PAA fiber is 126±3 μm.

### PEO/PAA-Dopa Fibers Preparation

PAA-Dopa (4.6 g) was dissolved in 50 mL of deionized water at room temperature under nitrogen atmosphere for 5 h. PEO (2.2 g) was dissolved in 60 mL of NaOH solution (0.75 mol·L$^{-1}$) at room temperature for 5 h. The PEO solution was added dropwise into the PAA-Dopa solution and stirred for 5 h under the nitrogen atmosphere (concentration 6.5 wt%). After removal of air bubbles, the solution was extruded through a 0.21 mm spinneret (single hole) into a 2.0 mol·L$^{-1}$ HCl coagulation bath to obtain fibers. The fibers were immersed into the acidic 1.0 mmol·L$^{-1}$ $NaIO_4$ solution (pH 2.0) for 6 h, then rinsed with acidic water (pH 2.0) to remove $NaIO_4$, and finally the PEO/PAA-Dopa fibers were spontaneous dry in ambient environment. The diameter of PEO/PAA-Dopa fiber is 151±5 μm.

### PEO/PAA-Dopa/Cu (Zn, Al or Fe) Fibers Preparation

The PEO/PAA-Dopa fibers were immersed in 1.5 mmol·L$^{-1}$ $CuCl_2$ solution (pH 3.0) for 3 h to form coordination bonds and then washed with acidic water to remove residual $CuCl_2$. The fiber was dried in ambient environment oven for 12 h. The preparation of PEO/PAA-Dopa/Zn, PEO/PAA-Dopa/Al, and PEO/PAA-Dopa/Fe fibers were prepared by immersing PAO/PAA-Dopa fibers into the corresponding solutions of zinc chloride (pH 3.0), aluminum chloride (pH 3.0), and ferric chloride (pH 2.0) solution with the concentration 1.5 mmol·L$^{-1}$, respectively. The flowing rinsing and drying processes were the same as that of PEO/PAA-Dopa/Cu fiber. The diameters of PEO/PAA-Dopa/Cu, PEO/PAA-Dopa/Zn, PEO/PAA-Dopa/Fe, and PEO/PAA-Dopa/Al fibers are 143±5, 140±6, 133±4, and 135±2 μm, respectively.

### Characterization and Testing

Fourier transform infrared (FTIR) spectra were recorded using Nicolet 8700 FT-IR spectrometer. PAA and PEO solid powder samples were mixed with KBr powder to press into a standard disk for FTIR measurements. The fiber samples were measured directly with attenuated total reflection (ATR, Single-Bounce) attachment. Metal ions ($Al^{3+}$, $Fe^{3+}$, $Zn^{2+}$ and $Cu^{2+}$) content in the fibers is measured with by inductively coupled plasma atomic emission spectrometry (ICP-AES, Prodigy Plus, Teledyne Leeman Labs).

Differential scanning calorimeter (DSC) was carried out using a 204 F differential scanning calorimeter manufactured by NETZSCH. The samples were heated from room temperature to 120 °C at a rate of 15 °C·min$^{-1}$, then cooled to −10 °C and heated again. The second heating curve was used to determine glass transition temperature.

The mechanical tensile testing of the single fiber was performed with a machine (XS(08)XG-3, mechanical sensor 50 cN) with a gap of 10 mm under relative humidity (RH) 65% at 25 °C. Before testing, all the fibers were incubated for 12 h to reach an equilibrium state in an automatically controlled humidity chamber (Testsky, Nanjing, China) at a designated humidity and temperature. During testing, different stretching rates were applied including 12, 40, 100, 200 and 400 mm·min$^{-1}$ (strain rates: 0.02, 0.07, 0.17, 0.33 and 0.66 s$^{-1}$). For the hysteresis testing, the consecutive loading-unloading cycles were performed from strain 100% to 800% with increment of 100% at a constant stretching rate 60 mm/min. For elastic recovery testing, the fiber was initially stretched to a predetermined strain (300%) and then unloaded at the same rate. After each cycle, the samples were relaxed at room temperature for different period (10 s–240 min) before the next loading process. The permanent set was defined by the ratio

https://doi.org/10.1007/s10118-023-2992-5

of the residual length along the direction of the force and the original length of the fiber.

## RESULTS AND DISCUSSION

PAA and PEO can form hydrogen-bonded polymer complex which exhibits rubber elastic behavior and mendable capacity.[18,30,53,54] PEO is semi-crystalline polymer and its chain is very flexible.[55] The glass transition temperature ($T_g$) of PEO is −60 °C.[56] Generally, PEO would not present rubber-like elastic properties due to high crystallization degree. PAA is amorphous polymer, $T_g$ of PAA is reported to 106−147 °C dependent on characterization methods.[18] PEO/PAA complex shows rubber-like behavior in ambient environment owing to hydrogen bonding complexation restricts the crystallization of PEO, hydrogen bonds provide dynamic cross-linking points, and water adsorption from the environment further improves polymer chain mobility.[30]

PEO/PAA complex has been shaped into fibers.[30,53] PEO/PAA complex fibers show highly elastic behaviors. However, PEO/PAA fibers are not stable. The fibers swell in neutral water and quickly dissolve in high pH solution (Fig. S4a in ESI). Here we apply catechol chemistry and coordination to stabilize and strengthen PEO/PAA fibers. Dopamine molecules are linked as side groups of PAA, and then it is combined with PEO to prepare the fibers which are treated with $NaIO_4$ to realize cross-linking of Dopa. These PEO/PAA-Dopa fibers are further immersed into $CuCl_2$, $ZnCl_2$, $AlCl_3$, or $FeCl_3$ solution to introduce coordination. Compared with PEO/PAA fibers, PEO/PAA-Dopa fibers and PEO/PAA-Dopa/Metal fibers do not dissolve in pH 14 and only slightly swollen after soaking for 7 days (Fig. S4b in ESI), indicating the improvement of stability.

Dopamine (Dopa) is a kind of catechol and has two phenol groups. Phenol can form hydrogen bond with PEO chain.[57] The linked Dopa can be further cross-linked through oxidation induced dismutation.[58] Moreover, carboxylate and catechol both have coordination capacity with different metal ions.[59] The resulting PEO/PAA-Dopa/metal fibers contain hydrogen bonds, coordinate bonds and covalent bonds cross-linkage, as shown in Fig. 1(a).

FTIR spectra of PAA, PEO and different fibers are shown in

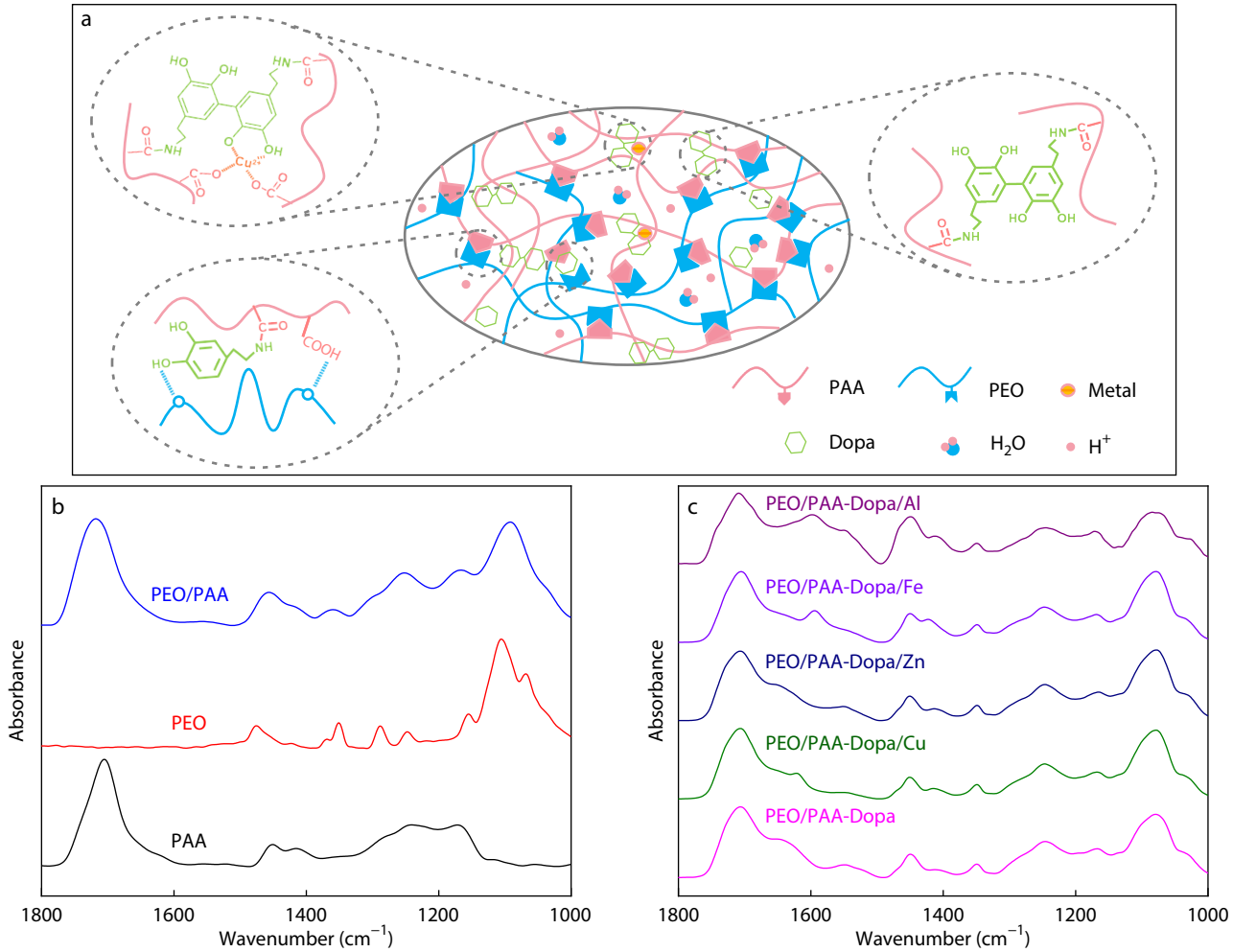


**Fig. 1** (a) The network structure of the PEO/PAA-Dopa/metal fibers. The FTIR spectra of (b) PEO/PAA fibers, PAA powder, PEO powder and (c) PEO/PAA-Dopa/Al, PEO/PAA-Dopa/Fe, PEO/PAA-Dopa/Zn, PEO/PAA-Dopa/Cu, and PEO/PAA-Dopa fibers (the spectra are intentionally overlaid for clarity).

https://doi.org/10.1007/s10118-023-2992-5

Figs. 1(b) and 1(c). The C=O band of neat PAA appears at 1704 $cm^{-1}$ and C—O—C band of neat PEO is at 1105 $cm^{-1}$.[53] The band of C=O from PEO/PAA fiber is located at 1718 $cm^{-1}$ and the band of C—O—C is 1090 $cm^{-1}$. For PEO/PAA fiber, there is hydrogen bonding between COOH and ether oxygen, which makes the absorbance band of C—O—C shift to the low wavenumber compared with PEO.[30] The C=O band of COOH in the PEO/PAA fiber moves to the high wavenumber in the contrast with pure PAA bulk because hydrogen bonding between COOH and ether oxygen completes with the hydrogen bonding among COOH for certain degree.[53]

FTIR spectrum of PEO/PAA-Dopa fiber shows difference compared with that of PEO/PAA fiber. The C=O band of PEO/PAA-Dopa is at 1706 $cm^{-1}$ and the band of C—O—C is at 1078 $cm^{-1}$. In the PEO/PAA-Dopa fiber, there are phenol groups which are hydrogen bonding donor too. Therefore, PEO/PAA-Dopa fiber present more hydrogen bonding interaction modes than PEO/PAA fiber does. When compared PEO/PAA-Dopa fiber with PEO/PAA-Dopa/Metal fibers, the major difference presents in the region of 1650–1500 $cm^{-1}$. The metal ions have coordination with carboxylate and phenol group, which would interrupt the hydrogen bonding, and hence IR adsorption band of the corresponding groups shift.[60] The spectra also reveal the carboxylate symmetric stretch ($\nu_{s(COO^-)}$) at 1415–1410 $cm^{-1}$, and the carboxylate asymmetric stretch ($\nu_{as(COO^-)}$) at 1594–1545 $cm^{-1}$. This is due to the ionization of carboxylic acid group during the complexation of Al, Fe, Cu, and Zn with PAA-Dopa.[61,62] The metal ion content in the fiber was determined by ICP-AES. The weight contents of Cu, Zn, Fe and Al in the corresponding fibers are 3.3 wt%, 3.1 wt%, 3.4 wt% and 2.9 wt%, respectively.

The stress-strain curves of PEO/PAA, PEO/PAA-Dopa, PEO/PAA-Dopa/Cu, PEO/PAA-Dopa/Zn, PEO/PAA-Dopa/Fe and PEO/PAA-Dopa/Al fibers are shown in Fig. 2(a). The mechanical parameters, initial modulus, tensile strength, ultimate strain, and toughness of these fibers are listed in Table 1. The pristine PEO/PAA fiber is soft and shows excellent stretchability. The initial modulus of PEO/PAA fiber is about 4 MPa. The ultimate strain of PEO/PAA fiber is about 1000%, which is higher than traditional elastomers, such as natural rubber and polyurethane.[20] Compared with PEO/PAA fiber, PEO/PAA-Dopa fiber remains soft, with low modulus and high elongation. These two curves diverge at the elongation strain around 500%. Before the failure, the PEO/PAA-Dopa fiber experienced distinct stiffening. Here, the stiffening is not only owning to the orientation induced hardening but also Dopa dismutation induced cross-linkage which resist the stress. The ultimate stress of the PEO/PAA-Dopa fiber is about 12 MPa while that of PEO/PAA fiber is only 3.5 MPa.

Four different metal ions are introduced into PEO/PAA-Dopa fibers separately. At 25 °C, RH 65%, PEO/PAA-Dopa/Al fiber shows brittle mechanical behavior, high initial modulus (~GPa), low ultimate strain (~8%), and failure without yielding. PEO/PAA-Dopa/Fe fiber shows yielding, but after yielding, the fiber quickly breaks. PEO/PAA-Dopa/Zn fiber exhibits ductile behavior. After yielding the stress of PEO/PAA-Dopa/Zn fiber suddenly decreases to the minimum value and then is followed with an obvious hardening. Among these four metal-ion-involved fibers, PEO/PAA-Dopa/Cu fiber is spe-

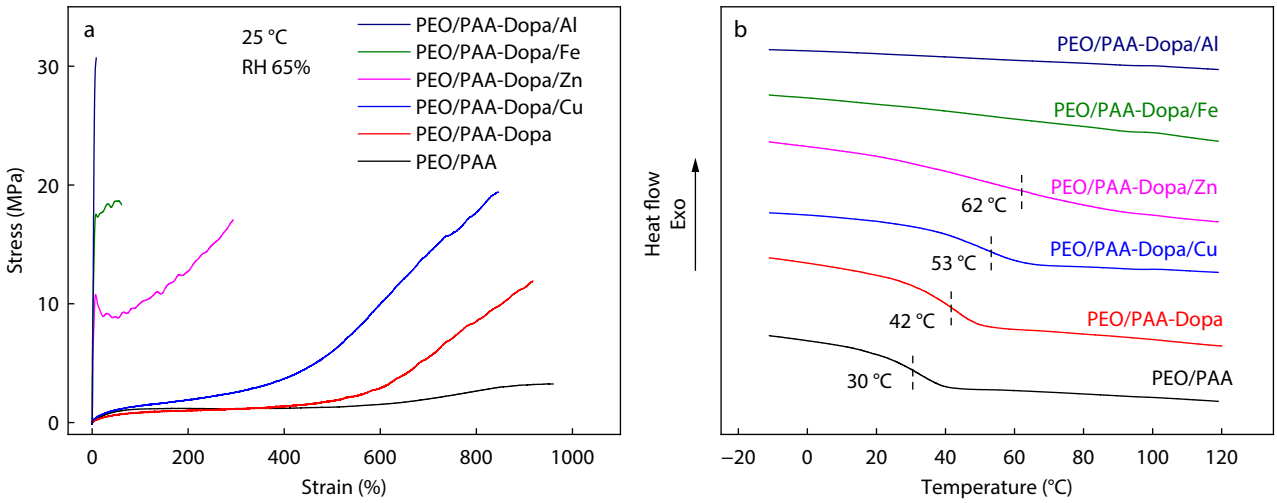


**Fig. 2** (a) Stress-strain curves and (b) the second heating DSC curves of PEO/PAA, PEO/PAA-Dopa, PEO/PAA-Dopa/Cu, PEO/PAA-Dopa/Zn, PEO/PAA-Dopa/Fe, and PEO/PAA-Dopa/Al fibers (stretching rate: 40 mm·$min^{-1}$, at 25 °C, RH 65%).

**Table 1** Mechanical properties of different fibers (25 °C, RH 65%).

| Sample | Initial modulus (MPa) | Tensile strength (MPa) | Ultimate strain (%) | Toughness (MJ·$m^{-3}$) |
|---|---|---|---|---|
| PEO/PAA | 4.1±0.2 | 3.5±0.1 | 960.2±15.5 | 15.0±1.2 |
| PEO/PAA-Dopa | 2.9±0.1 | 12.0±0.3 | 917.6±12.3 | 30.0±0.9 |
| PEO/PAA-Dopa/Cu | 7.0±0.7 | 19.4±0.4 | 845.9±20.4 | 57.0±1.5 |
| PEO/PAA-Dopa/Zn | 429.0±3.3 | 17.0±0.3 | 293.6±7.3 | 34.0±1.1 |
| PEO/PAA-Dopa/Fe | 678.0±4.2 | 18.5±0.5 | 60.1±5.2 | 10.0±0.7 |
| PEO/PAA-Dopa/Al | 1049.0±3.7 | 31.0±0.6 | 8.6±1.0 | 1.7±0.2 |

https://doi.org/10.1007/s10118-023-2992-5

cial. PEO/PAA-Dopa/Cu fiber keeps the elastic behavior like its precursor fiber, but has the higher initial modulus and ultimate strength. The toughness of PEO/PAA-Dopa/Cu fiber is the highest among all these fibers, including its precursor fibers (PEO/PAA and PEO/PAA-Dopa) and its metal-involved counterpart fibers (PEO/PAA-Dopa/Zn, PEO/PAA-Dopa/Fe, and PEO/PAA-Dopa/Al), as shown in Table 1. In PEO/PAA-Dopa/Cu fiber, interchain hydrogen bonding, covalent bond cross-linking, and coordination have good synergy, which provide the mechanism of energy dissipation at different stretch stage and make the fiber be endowed with high toughness.

Glass transition temperature ($T_g$) is an indicator to the polymer segment mobility. To correlate the mechanical properties of the fibers with chain segment mobility, we used DSC to measure $T_g$s the of these fibers in dry state (Fig. 2b). Dry PEO/PAA fiber shows $T_g$ at 30 °C. The detected $T_g$ of the dry PEO/PAA-Dopa fiber is 42 °C, which is higher than that of PEO/PAA fiber, due to the cross-linking of Dopa. DSC do not detect the glass transitions of PEO/PAA-Dopa/Fe and PEO/PAA-Dopa/Al fibers until to 120 °C. These two fibers present the brittle mechanical behaviors at the room temperature. $T_g$s of the dry PEO/PAA-Dopa/Cu and PEO/PAA-Dopa/Zn fibers are 53 and 62 °C, respectively. At 25 °C RH 65%, PEO/PAA-Dopa/Zn fiber shows ductile behavior while PEO/PAA-Dopa/Cu fiber presents rubber behavior, owing to the adsorbed water from the environment acted as the plasticizer in the fibers.

The mechanical behaviors of PEO/PAA-Dopa/Cu fiber at different humidities are shown in Fig. 3(a). The water content is the water absorption weight of fiber versus wet weight of fiber, and water contents in the fibers after incubation in relative humidity (RH) 40%, 55%, 65% and 90% at 25 °C are 2.7%, 5.2%, 7.3% and 16.0%, respectively. The completely dry PEO/PAA-Dopa/Cu fiber is brittle. As the humidity increased, PEO/PAA-Dopa/Cu fiber transfers from rigid glass to flexible

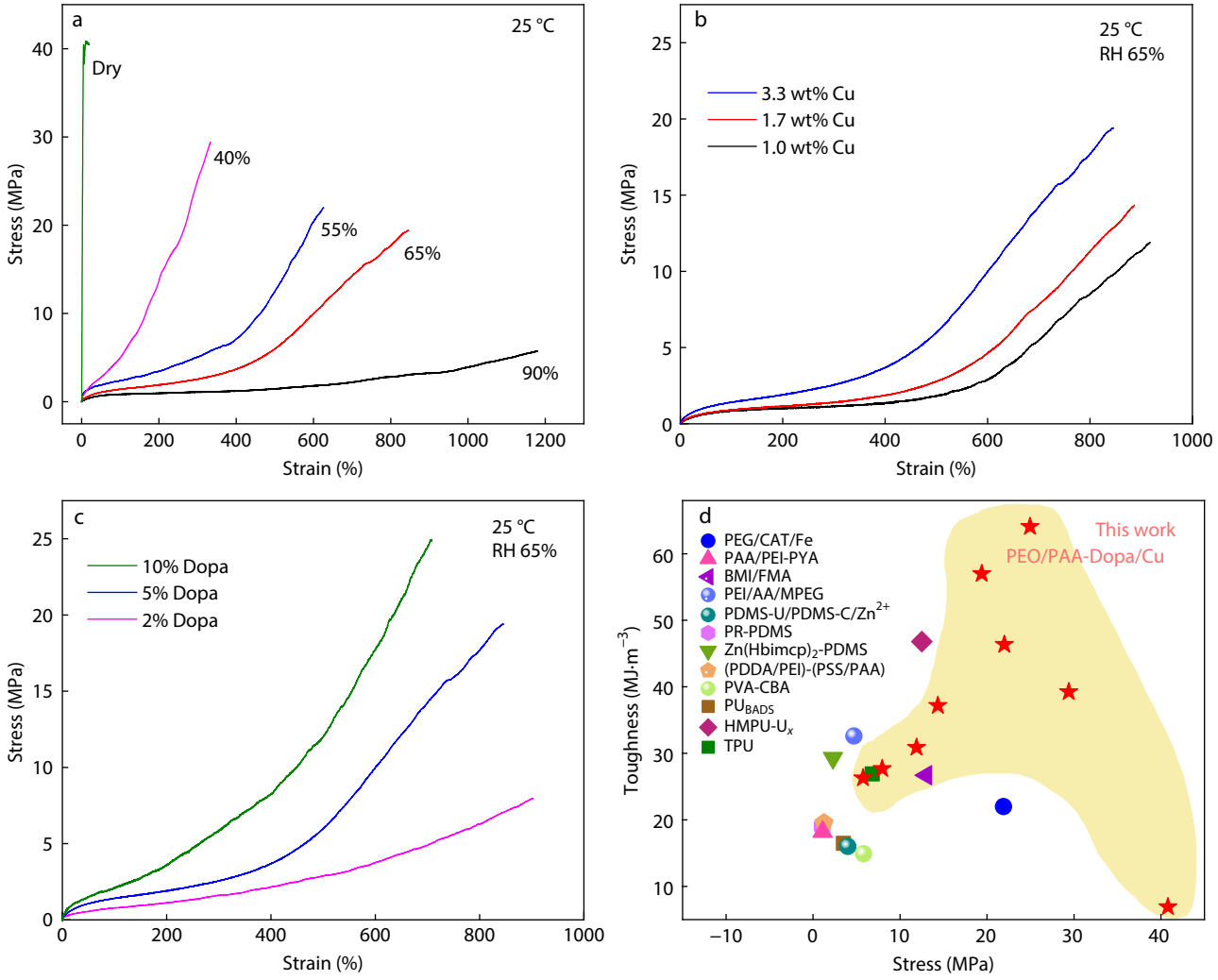


**Fig. 3** (a) Stress-strain curves of PEO/PAA-Dopa/Cu fibers at different humidities (stretching rate: 40 mm·min$^{-1}$ at 25 °C); (b) Stress-strain curves of PEO/PAA-Dopa/Cu fibers prepared with different weight contents of Cu; (c) Stress-strain curves of PEO/PAA-Dopa/Cu fibers with different Dopa grafting ratios; (d) Ashby diagrams of toughness versus ultimate tensile strength of PEO/PAA-Dopa/Cu complex elastic fibers and other reported polymeric elastomers and hydrogels (PEG/CAT/Fe,[50] PAA/PEI-PYA,[63] BMI/FMA,[64] PEI/AA/MPEG,[65] PDMS-U/PDMS-C/$Zn^{2+}$,[66] PR-PDMS,[67] $Zn(Hbimcp)_2$-PDMS,[68] (PDDA/PEI)-(PSS/PAA),[69] PVA-CBA,[70] $PU_{BADS}$,[71] HMPU-$U_x$,[72] and TPU[73]).

https://doi.org/10.1007/s10118-023-2992-5

elastomer. At RH 90%, the ultimate strain and stress of PEO/PAA-Dopa/Cu fiber are about 1200% and 5.7 MPa, respectively. PEO/PAA-Dopa/Cu fiber inherits mendable capability from PEO/PAA complex. After being cut into two pieces, PEO/PAA-Dopa/Cu fiber can partially recover its mechanical strength. After bringing two surfaces of the freshly cut fiber to contact at humid environment (RH 90% at 25 °C), the fiber is able to support a stress of 2 MPa after 15 min, and shows a tensile strength of 4 MPa after 6 h (Fig. S5 in ESI). Cutting breaks both covalent bonds and non-covalent bonds. Non-covalent bonds can recover under proper condition while the covalent bonds cannot. For PEO/PAA-Dopa/Cu fiber, though the covalent cross-linkages does not self-healing, hydrogen bonding and coordination can re-form at the contacted interface, and hence the fiber remains certain mendable capacity.

We further investigated the mechanical properties of PEO/PAA-Dopa/Cu fiber with different $Cu^{2+}$ ions concentrations (Fig. 3b) or different Dopa grafting ratios (Fig. 3c). Either as $Cu^{2+}$ content or dopamine grafting degree increases, the ultimate strength and initial modulus of the fiber will improve. As more $Cu^{2+}$ ion introduced into fiber, more coordination cross-linking points will produce. As Dopa grafting degree increases, that more covalent bond cross-linking points will form. It illustrates that the modulus and the strength of polymeric network show dependency on the cross-linking density.[45]

Figs. 3(a)–3(c) clearly demonstrate that the mechanical properties of PEO/PAA-Dopa/Cu fiber can be finely adjusted by the environmental humidity, $Cu^{2+}$ ion content, and Dopa grafting degree. PEO/PAA-Dopa/Cu fiber has the synergy of hydrogen bonds, coordination bonds and covalent bonds, and shows capacity to adjust its mechanical properties in wide range. The Ashby diagram of toughness versus ultimate tensile strength of PEO/PAA-Dopa/Cu fiber is constructed, as shown in Fig. 3(d). The ultimate strength of PEO/PAA-Dopa/Cu fiber ranges from 6 MPa to 41 MPa, and its toughness varies from 7 MJ·m$^{-3}$ to 64 MJ·m$^{-3}$. Other reported elastomer or hydrogel systems are also exhibited in the Ashby diagram (Fig. 3d). The toughness of double reversible network,[63–66] sliding cross-linking,[67] and covalent bond and dynamic bond,[50,68–73] are reported as 33, 19 and 47 MJ·m$^{-3}$, respectively. PEO/PAA-Dopa/Cu fiber will present toughness more than 60 MJ·m$^{-3}$ under proper condition, which are higher than these reported elastomers and hydrogels.

## Strain Rate Dependency

To further study the dynamic network of PEO/PAA-Dopa/Cu fiber, the tensile tests with different stretching rate were performed, as shown in Fig. 4(a). Through the slope (*i.e.*, modulus) of the stress-strain curve of PEO/PAA-Dopa/Cu fiber, the tensile curve is divided into three regions, initial linear region (I), rubber plateau (II), and hardening region (III), as shown in Fig. S6 (in ESI). The fiber shows different modulus at these three regions. The region I has the highest modulus, the region II has the lowest, and the region III has the medium (Fig. 4b).

The modulus of the region I and the region II both show dependence on the strain rate while the region III does not. These strain rate dependent behaviors reflect different relaxation time scales of the network in PEO/PAA-Dopa/Cu fiber.[42] In initial elastic region (I) and rubber plateau (II) the breakage of hydrogen bonds and coordination support the elongation of the fiber, the related relaxation processes match the experimental strain rate, and hence the modulus in these two regions exhibit the dependence on strain rate. At the large strain, the fiber bears the higher stress. The covalent cross-linkages resist the stress in this hardened zone, and the modulus does not show dependence on the strain rate. Hydrogen bonds play a leading role in initial elastic region I, the coordination bonds enhance the modulus in rubber plateau II, and covalent bonds resist the stress in hardening region III. The synergy of the three interactions ensures the mechanical strength and toughness of the fiber.

## Hysteresis

The three-dimensional network containing hydrogen bonding, coordination bond, and covalent cross-linking allows the fiber to resist the stress and dissipate energy at different length scales. To quantify the efficiency of energy dissipation of these fibers,

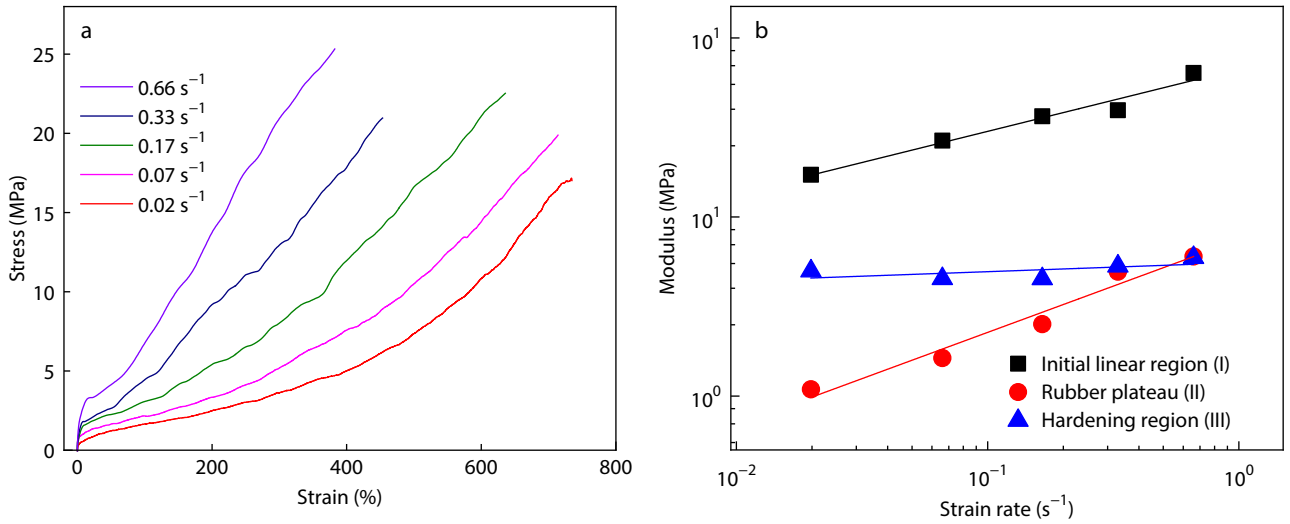


**Fig. 4** (a) Stress-strain curves of PEO/PAA-Dopa/Cu fibers at different strain rates; (b) Young's modulus of the PEO/PAA-Dopa/Cu fiber at different strain rates in three different regions.

https://doi.org/10.1007/s10118-023-2992-5

we performed cyclic tensile tests with different strain, stepwise increasing from 100% to 800%. PEO/PAA, PEO/PAA-Dopa, and PEO/PAA-Dopa/Cu fibers all show obvious hysteresis in loading-unloading cycle, as shown in Fig. 5. Hysteresis is due to energy dissipation. The energy dissipation ratio is defined as the integrated area in the hysteresis loop versus the area under the loading curve.[14] As the strain becomes large, the energy dissipation ratio of PEO/PAA-Dopa fiber will increase. However, the energy dissipation ratio of PEO/PAA or PEO/PAA-Dopa/Cu fiber does not sensitive to the strain increasing. Among these three fibers, PEO/PAA-Dopa/Cu fiber exhibits the highest energy dissipation ratio, about 60%. The energy dissipation of PEO/PAA fiber is about 30%. It demonstrated that introducing coordination can significantly enhance the energy dissipation.

## Permanent Set and Recovery

The fibers are performed with loading-unloading cycles with the fixed strain (300%). We gradually increased the resting time between the two successive cycles. The loading-unloading curves of PEO/PAA fiber, PEO/PAA-Dopa fiber and PEO/PAA-Dopa/Cu fiber are shown in Figs. 6(a)–6(c). All three fibers show recovery, and as the resting time prolongs the recovery degree will increase. The permanent set is defined the ratio of the unrecovered the residual length versus the original length of the fiber. As shown in Fig. 6(d), the permanent set will become smaller as the resting time prolongs.

PEO/PAA-Dopa/Cu fiber shows much quicker reduction of the permanent set than PEO/PAA or PEO/PAA-Dopa fiber does. With 10 min resting, the permanent set of PEO/PAA-Dopa/Cu fiber is close to 0. However, PEO/PAA and PEO/PAA-Dopa fiber need at least 4 h. It means that after removing loading force, PEO/PAA-Dopa/Cu fiber can almost recover its original length in 10 min while PEO/PAA and PEO/PAA-Dopa fiber recover more than 4 h. It demonstrates that introduction of the coordination can accelerate the length recovery for the fiber.

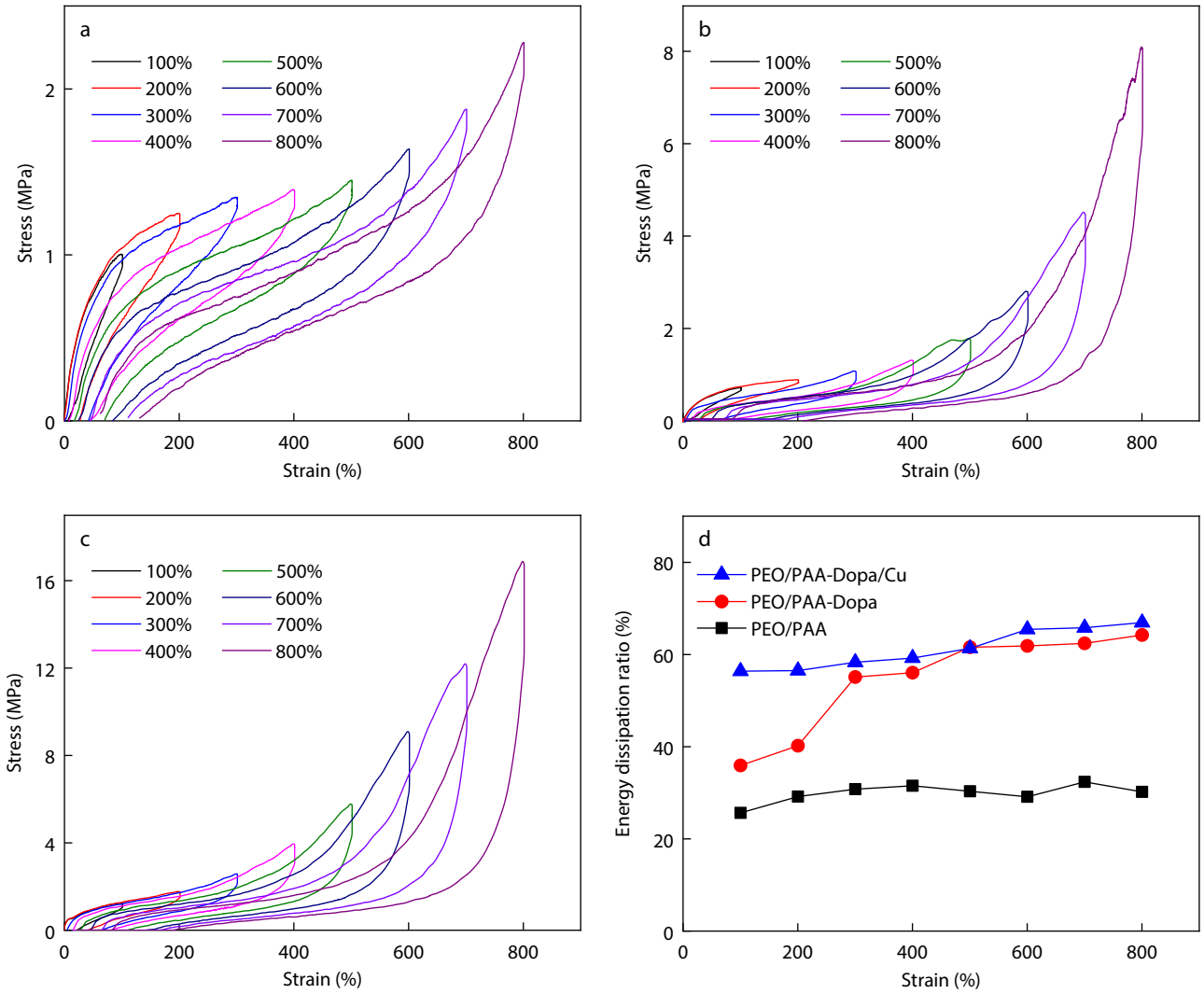


**Fig. 5** (a) PEO/PAA fibers, (b) PEO/PAA-Dopa fibers and (c) PEO/PAA-Dopa/Cu fibers in cyclic tensile loading-unloading curves under different strains (100%–800%) at room temperature (stretching rate: 60 mm·min$^{-1}$), and (d) energy dissipation ratio of different fibers as function of the strain.

https://doi.org/10.1007/s10118-023-2992-5

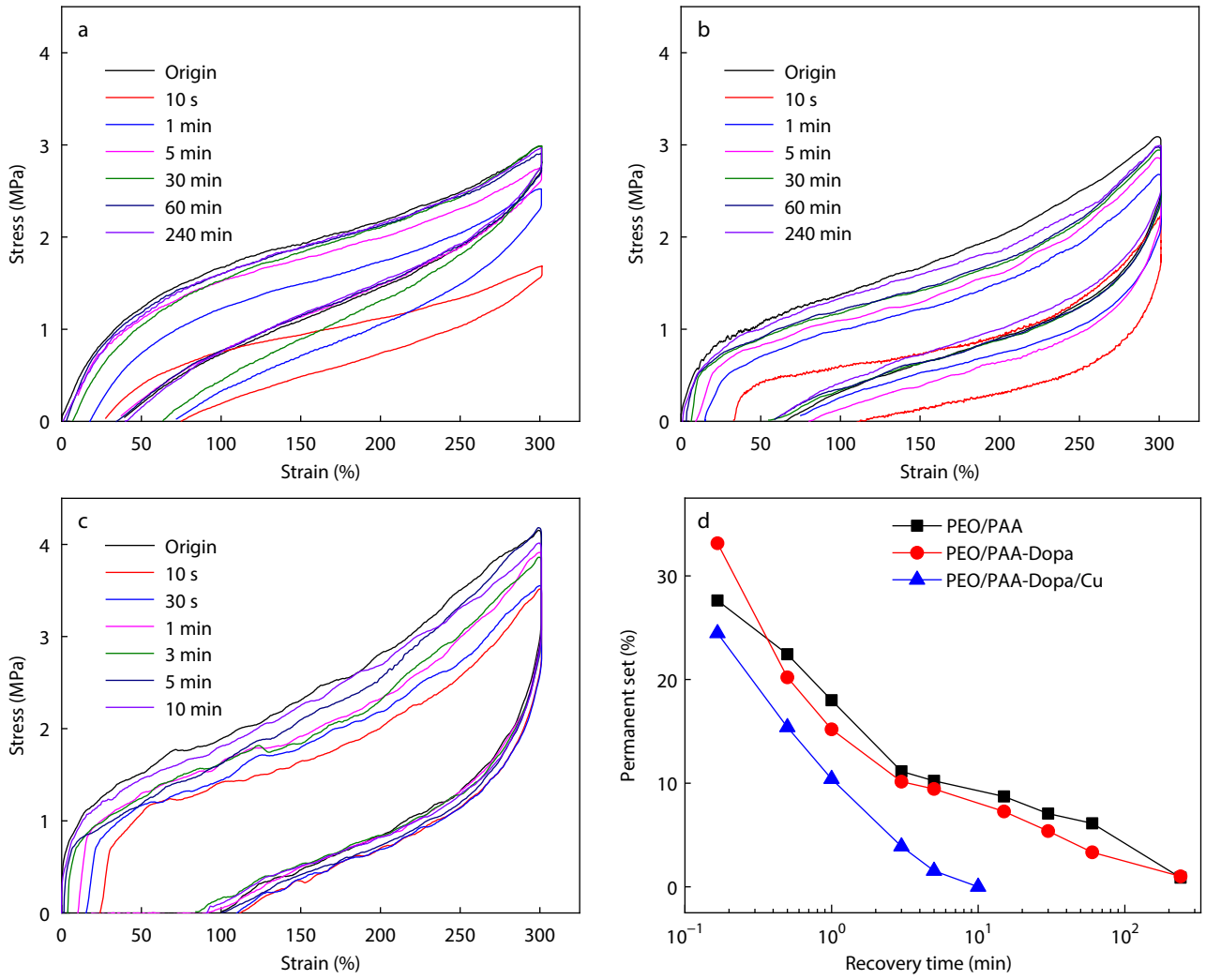


**Fig. 6** Cycle loading-unloading curves of (a) PEO/PAA fibers, (b) PEO/PAA-Dopa fibers and (c) PEO/PAA-Dopa/Cu fibers with the fixed strain (300%) and different resting time between two cycles, and (d) permanent set as a function of resting times between two loading-unloading cycles. (Stretching rate: 100 mm·min$^{-1}$ at 25 °C.)

## CONCLUSIONS

In summary, catechol chemistry and coordination successfully stabilize and strengthen the hydrogen-bonded polymer complex fiber of PEO and PAA. Compared with the precursor PEO/PAA fiber, PEO/PAA-Dopa/Cu fiber keeps extensibility, certain mendable ability and humidity sensitivity. More importantly, PEO/PAA-Dopa/Cu fiber has the higher stiffness, strength and toughness, and faster recovery with its precursor fibers.

Modification using Dopa and metal ions, the fibers contain hydrogen bonds, coordination and covalent cross-linking. Hydrogen-bonding and coordination, which are dynamic and reversible, effectively dissipate the applied energy during the deformation process, while covalent cross-linking resists the stress at large strain and provides enough recovery force after removing stress. The synergy of hydrogen bonds, coordination and covalent cross-linking endows the fiber with stability, rubber elasticity and toughness.

### Conflict of Interests

The authors declare no interest conflict.

### Electronic Supplementary Information

Electronic supplementary information (ESI) is available free of charge in the online version of this article at http://doi.org/10.1007/s10118-023-2992-5.

## ACKNOWLEDGMENTS

This work was financially supported by the National Natural Science Foundation of China (Nos. 51973029 and 52273020) and Ministry of Education (No. 8091B022141).

## REFERENCES

1 Boretos, J. W.; Pierce, W. S. Segmented polyurethane: a new

elastomer for biomedical applications. *Science* **1967**, *158*, 1481–1482.
2 Chen, Y.; Miller, P.; Ding, X.; Stowell, C.; Kelly, K.; Wang, Y. Chelation crosslinking of biodegradable elastomers. *Adv. Mater.* **2020**, *32*, 2003761.
3 Li, Z. Q.; Zhu, Y. L.; Niu, W. W.; Yang, X.; Jiang, Z. Y.; Lu, Z. Y.; Liu, X. K.; Sun, J. Q. Healable and recyclable elastomers with record-high mechanical robustness, unprecedented crack tolerance, and superhigh elastic restorability. *Adv. Mater.* **2021**, *33*, 2101498.
4 Lei, W. W.; Zhou, X. X.; Russell, T. P.; Hua, K. C.; Yang, X. P.; Qiao, H.; Wang, W. C.; Li, F. Z.; Wang, R. G.; Zhang, L. Q. High performance bio-based elastomers: energy efficient and sustainable materials for tires. *J. Mater. Chem. A* **2016**, *4*, 13058–13062.
5 Le Floch, P.; Yao, X.; Liu, Q. H.; Wang, Z. J.; Nian, G. D.; Sun, Y.; Jia, L.; Suo, Z. G. Wearable and washable conductors for active textiles. *ACS Appl. Mater. Interfaces* **2017**, *9*, 25542–25552.
6 Vatankhah-Varnosfaderani, M.; Keith, A. N.; Cong, Y. D.; Liang, H. Y.; Rosenthal, M.; Sztucki, M.; Clair, C.; Magonov, S.; Ivanov, D. A.; Dobrynin, A. V.; Sheiko, S. S. Chameleon-like elastomers with molecularly encoded strain-adaptive stiffening and coloration. *Science* **2018**, *359*, 1509–1513.
7 Ohm, C.; Brehmer, M.; Zentel, R. Liquid crystalline elastomers as actuators and sensors. *Adv. Mater.* **2010**, *22*, 3366–3387.
8 Sheiko, S. S.; Dobrynin, A. V. Architectural code for rubber elasticity: from supersoft to superfirm materials. *Macromolecules* **2019**, *52*, 7531–7546.
9 Cordier, P.; Tournilhac, F.; Soulie-Ziakovic, C.; Leibler, L. Self-healing and thermoreversible rubber from supramolecular assembly. *Nature* **2008**, *451*, 977–980.
10 Ducrot, E.; Chen, Y. L.; Bulters, M.; Sijbesma, R. P.; Creton, C. Toughening elastomers with sacrificial bonds and watching them break. *Science* **2014**, *344*, 186–189.
11 Jiang, F.; Fang, C.; Zhang, J.; Wang, W. T.; Wang, Z. G. Triblock copolymer elastomers with enhanced mechanical properties synthesized by RAFT polymerization and subsequent quaternization through incorporation of a comonomer with imidazole groups of about 2.0 mass percentage. *Macromolecules* **2017**, *50*, 6218–6226.
12 Wang, W. J.; Zhang, C. H.; Huang, H.; Liu, Z. X. Jian, H. X.; Yang, S. G. Combining microphase separation and hydrogen-bonding complexation to construct elastomer. *Acta Polymerica Sinica* (in Chinese) **2023**, *54*, 478–486.
13 Yasui, T.; Zheng, Y.; Nakajima, T.; Kamio, E.; Matsuyama, H.; Gong, J. P. Rate-independent self-healing double network hydrogels using a thixotropic sacrificial network. *Macromolecules* **2022**, *55*, 9547–9557.
14 Wu, J. R.; Cai, L. H.; Weitz, D. A. Tough self-healing elastomers by molecular enforced integration of covalent and reversible networks. *Adv. Mater.* **2017**, *29*, 1702616.
15 Guo, H. S.; Han, Y.; Zhao, W. Q.; Yang, J.; Zhang, L. Universally autonomous self-healing elastomer with high stretchability. *Nat. Commun.* **2020**, *11*, 2037.
16 Wang, D; Xu, J. H.; Chen, J. Y.; Hu, P.; Wang, Y.; Jiang, W.; Fu, J. J. Transparent, mechanically strong, extremely tough, self-recoverable, healable supramolecular elastomers facilely fabricated *via* dynamic hard domains design for multifunctional applications. *Adv. Funct. Mater.* **2020**, *30*, 1907109.
17 Wu, X. Z.; Wang, J. Q.; Huang, J. X.; Yang, S. R. Robust, stretchable, and self-healable supramolecular elastomers synergistically cross-linked by hydrogen bonds and coordination bonds. *ACS Appl. Mater. Interfaces* **2019**, *11*, 7387–7396.
18 Wang, Y.; Liu, X.; Li, S.; Li, T.; Song, Y.; Li, Z.; Zhang, W.; Sun, J. Q. Transparent, healable elastomers with high mechanical strength and elasticity derived from hydrogen-bonded polymer complexes. *ACS Appl. Mater. Interfaces* **2017**, *9*, 29120–29129.
19 Wang, W. Y.; Lu, W.; Goodwin, A.; Wang, H. Q.; Yin, P. C.; Kang, N. G.; Hong, K. L.; Mays, J. W. Recent advances in thermoplastic elastomers from living polymerizations: macromolecular architectures and supramolecular chemistry. *Prog. Polym. Sci.* **2019**, *95*, 1–31.
20 Hu, J. L.; Lu, J.; Zhu, Y. New developments in elastic fibers. *Polym. Rev.* **2008**, *48*, 275–301.
21 Nurhamiyah, Y.; Amir, A.; Chen, B. Q. Wholly biobased, highly stretchable, hydrophobic, and self-healing thermoplastic elastomer. *ACS Appl. Mater. Interfaces* **2021**, *13*, 6720–6730.
22 Zhu, M. M.; Wang, W. J.; Zhang, C. H.; Zhu, L. P.; Yang, S. G. Photo-responsive behaviors of hydrogen-bonded polymer complex fibers containing azobenzene functional groups. *Adv. Fiber Mater.* **2021**, *3*, 172–179.
23 Yu, J. C.; Chen, K.; Ji, H.; Zhang, Y.; Zhang, Y. M.; Pan, Z. J. Facile and large-scale fabrication of self-crimping elastic fibers for large strain sensors. *Chinese J. Polym. Sci.* **2021**, *39*, 914–924.
24 Chen, M. X.; Wang, Z.; Li, K. W.; Wang, X. D.; Wei, L. Elastic and stretchable functional fibers: a review of materials, fabrication methods, and applications. *Adv. Fiber Mater.* **2021**, *3*, 1–13.
25 Ziabichi, A., in *Fundamentals of Fiber Formation*, John Wiley &Sons: London, **1976**, Chapter 5.
26 Casey, P.; Chen, H. Y.; Poon, B.; Bensason, S.; Menning, B.; Liu, L. Z.; Hu, Y. S.; Hoenig, W.; Gelfer, M.; Dems, B.; Rego, M. Polyolefin based crosslinked elastic fiber: a technical review of DOW XLA™ elastic fiber technology. *Polym. Rev.* **2008**, *48*, 302–316.
27 Lee, S.; Shin, S.; Lee, S.; Seo, J.; Lee, J.; Son, S.; Cho, H. J.; Algadi, H.; Al-Sayari, S.; Kim, D. E.; Lee, T. Ag nanowire reinforced highly stretchable conductive fibers for wearable electronics. *Adv. Funct. Mater.* **2015**, *25*, 3114–3121.
28 Hicks, E. M. J.; Ultee, A. J.; Drougas, J. Spandex elastic fibers: Development of a new type of elastic fiber stimulates further work in the growing field of stretch fabrics. *Science* **1965**, *147*, 373–379.
29 Ma, R.; Kang, B.; Cho, S.; Choi, M.; Baik, S. Extraordinarily high conductivity of stretchable fibers of polyurethane and silver nanoflowers. *ACS Nano* **2015**, *9*, 10876–10886.
30 Li, J. F.; Wang, Z. L.; Wen, L. G.; Nie, J.; Yang, S. G.; Xu, J. Cheng, S. Z. D. Highly elastic fibers made from hydrogen-bonded polymer complex. *ACS Macro Lett.* **2016**, *5*, 814–818.
31 Wang, W. J.; Xu, X.; Zhang, C. H.; Huang, H.; Zhu, L. P.; Yue, K.; Zhu, M. F.; Yang, S. G. Skeletal muscle fibers inspired polymeric actuator by assembly of triblock polymers. *Adv. Sci.* **2022**, *9*, 2105764.
32 Liu, D. Z.; Zhu, L. P.; Huang, W. T.; Yue, K.; Yang, S. G. Polymer complex fiber for linear actuation with high working density and stable catch-state. *ACS Macro Lett.* **2020**, *9*, 1507–1513.
33 Niu, W. W.; Zhu, Y. L.; Wang, R.; Lu, Z. Y.; Liu, X. K.; Sun, J. Q. Remalleable, healable, and highly sustainable supramolecular polymeric materials combining superhigh strength and ultrahigh toughness. *ACS Appl. Mater. Interfaces* **2020**, *12*, 30805–30814.
34 Bokobza, L. The reinforcement of elastomeric networks by fillers. *Macromol. Mater. Eng.* **2004**, *289*, 607–621.
35 Heinrich, G.; Kluppel, M.; Vilgis, T. A. Reinforcement of elastomers. *Curr. Opin. Solid State Mater. Sci.* **2002**, *6*, 195–203.
36 Creton, C. 50th Anniversary perspective: networks and gels: soft but dynamic and tough. *Macromolecules* **2017**, *50*, 8297-8316.
37 Gong, J. P.; Katsuyama, Y.; Kurokawa, T.; Osada, Y. Double-network hydrogels with extremely high mechanical strength. *Adv. Mater.* **2003**, *15*, 1155–1158.
38 Hu, J.; Hiwatashi, K.; Kurokawa, T.; Liang, S. M.; Wu, Z. L.; Gong, J. P. Microgel-reinforced hydrogel films with high mechanical strength and their visible mesoscale fracture structure. *Macromolecules* **2011**, *44*, 7775–7781.
39 Li, H. J.; Zheng, H.; Tan, Y. J.; Tor, S. B. Zhou, K. Development of an ultrastretchable double-network hydrogel for flexible strain sensors. *ACS Appl. Mater. Interfaces* **2021**, *13*, 12814–12823.
40 Feng, J. F.; Chen, Z. H.; Fan, S. T.; Yu, L. P.; Tan, M.; Liao, L. G.; Li, B. J.; Zhang, S. Bioinspired ultra tear-resistant elastomer with a slidable double-network structure. *ACS Appl. Mater. Interfaces* **2022**, *14*, 31424–31434.
41 Zhang, N.; Pang, Y.; Li, Z. H.; Yang, C. H.; Zong, L.; Yang, H. S.; Wu, H.; Duan, Y. X.; Zhang, J. M. Rubber-like and biodegradable

poly(vinyl alcohol) composites with triple networks for high-efficiency solvent barrier. *Compos. Sci. Technol.* **2023**, *231*, 109801.
42 Lu, H. F.; Wang, M.; Chen, X. M.; Lin, B. P.; Yang, H. Interpenetrating liquid-crystal polyurethane/polyacrylate elastomer with ultrastrong mechanical property. *J. Am. Chem. Soc.* **2019**, *141*, 14364–14369.
43 Kang, J. H.; Son, D.; Wang, G. J. N.; Liu, Y. X.; Lopez, J.; Kim, Y.; Oh, J. Y.; Katsumata, T.; Mun, J. W.; Lee, Y. Tough and water-insensitive self-healing elastomer for robust electronic skin. *Adv. Mater.* **2018**, *30*, 1706846.
44 Voorhaar, L.; Diaz, M. M.; Leroux, F.; Rogers, S.; Abakumov, A. M.; Van Tendeloo, G.; Van Assche, G.; Van Mele, B.; Hoogenboom, R. Supramolecular thermoplastics and thermoplastic elastomer materials with self-healing ability based on oligomeric charged triblock copolymers. *NPG Asia Mater.* **2017**, *9*, e385.
45 Zhao, X. H. Multi-scale multi-mechanism design of tough hydrogels: building dissipation into stretchy networks. *Soft Matter* **2014**, *10*, 672–687.
46 Yin, Q. Y.; Dai, C. H.; Chen, H.; Gou, K.; Guan, H. Z.; Wang, P. H.; Jiang, J. T.; Weng, G. S. Tough double metal-ion cross-linked elastomers with temperature-adaptable self-healing and luminescence properties. *Chinese J. Polym. Sci.* **2021**, *39*, 554–565.
47 Krogsgaard, M.; Nue, V.; Birkedal, H. Mussel-inspired materials: Self-healing through coordination chemistry. *Chem. Eur. J.* **2016**, *22*, 844–857.
48 Bentley, W. E.; Payne, G. F. Nature's other self-assemblers. *Science* **2013**, *341*, 136–137.
49 Azevedo, S.; Costa, A. M. S.; Andersen, A.; Choi, I. S.; Birkedal, H.; Mono, J. F. Bioinspired ultratough hydrogel with fast recovery, self-healing, injectability and cytocompatibility. *Adv. Mater.* **2017**, *29*, 1700759.
50 Filippidi, E.; Cristiani, T. R.; Eisenbach, C. D.; Waite, J. H.; Israelachvili, J. N.; Ahn, B. K.; Valentine, M. T. Toughening elastomers using mussel-inspired iron-catechol complexes. *Science* **2017**, *358*, 502–505.
51 Liao, J. X.; Huang, J. H.; Wang, T.; Sun, W. X.; Tong, Z. Rapid shape memory and pH-modulated spontaneous actuation of dopamine containing hydrogels. *Chinese J. Polym. Sci.* **2017**, *35*, 1297–1306.
52 Wu, J. J.; Zhang, L.; Wang, Y. X.; Long, Y. H.; Gao, H.; Zhang, X. L.; Zhao, N.; Cai, Y. L.; Xu, J. Mussel-inspired chemistry for robust and surface-modifiable multilayer films. *Langmuir* **2011**, *27*, 13684–13691.
53 Nie, J.; Wang, Z. L.; Li, J. F.; Gong, Y.; Sun, J. X.; Yang, S. G. Interface hydrogen-bonded core-shell nanofibers by coaxial electrospinning. *Chinese J. Polym. Sci.* **2017**, *35*, 1001–1008.
54 Lutkenhaus, J. L.; Hrabak, K. D.; McEnnis, K.; Hammond, P. T. Elastomeric flexible free-standing hydrogen-bonded nanoscale assemblies. *J. Am. Chem. Soc.* **2005**, *127*, 17228–17234.
55 Cheng, S.; Chen, J. H.; Barley, J. S.; Zhang, A. Q.; Habenschuss, A.; Zschack, P. R. Isothermal thickening and thinning processes in low molecular-weight poly(ethylene oxide) fractions crystallized from the melt. 3. Molecular weight dependence. *Macromolecules* **1992**, *25*, 1453–1460.
56 Cheng, S.; Zhang, A. Q.; Barley, J. S.; Chen, J. H.; Habenschuss, A.; Zschack, P. R. Isothermal thickening and thinning processes in low-molecular-weight poly(ethylene oxide) fractions. 1. From nonintegral-folding to integral-folding chain crystal transitions. *Macromolecules* **1991**, *24*, 3937–3944.
57 Li, J. F.; Sun, J. X.; Wu, D.; Huang, W. T.; Zhu, M. F.; Reichmanis, E.; Yang, S. G. Functionalization-directed stabilization of hydrogen-bonded polymer complex fibers: elasticity and conductivity. *Adv. Fiber Mater.* **2019**, *1*, 71–81.
58 Sun, J. X.; Su, C.; Zhang, X. J.; Yin, W. J.; Xu, J.; Yang, S. G. Reversible swelling-shrinking behavior of hydrogen-bonded free-standing thin film stabilized by catechol reaction. *Langmuir* **2015**, *31*, 5147–5154.
59 Shi, L. Y.; Ding, P. H.; Wang, Y. Z.; Zhang, Y.; Ossipov, D.; Hilborn, J. Self-healing polymeric hydrogel formed by metal-ligand coordination assembly: design, fabrication, and biomedical applications. *Macromol. Rapid Commun.* **2019**, *40*, 1800837.
60 Sever, M. J.; Weisser, J. T.; Monahan, J.; Srinivasan, S.; Wilker, J. J. Metal-mediated cross-linking in the generation of a marine-mussel adhesive. *Angew. Chem.* **2004**, *116*, 454–456.
61 Auvil, N. C.; De Vasquez, M. G. V.; Allen, H. C. Zinc-carboxylate binding in mixed octadecanoic acid and octadecanol monolayers on proxy seawater solution surfaces. *ACS Earth Space Chem.* **2021**, *5*, 2947–2956.
62 El-Sawy, N. M.; Al Sagheer, F. Radiation-induced graft polymerization of acrylic acid onto poly(tetrafluoroethylene-perfluorovinyl ether) copolymer films: complexation with some transition metals and biological activity. *Eur. Polym. J.* **2001**, *37*, 161–166.
63 Yuan, T.; Qu, X. X.; Cui, X. M.; Sun, J. Q. Self-healing and recyclable hydrogels reinforced with in situ-formed organic nanofibrils exhibit simultaneously enhanced mechanical strength and stretchability. *ACS Appl. Mater. Interfaces* **2019**, *11*, 32346–32353.
64 Peng, Y.; Yang, Y.; Wu, Q.; Wang, S. X.; Huang, G. S.; Wu, J. R. Strong and tough self-healing elastomers enabled by dual reversible networks formed by ionic interactions and dynamic covalent bonds. *Polymer* **2018**, *157*, 172–179.
65 Fang, X.; Sun, J. Q. One-step synthesis of healable weak-polyelectrolyte-based hydrogels with high mechanical strength, toughness, and excellent self-recovery. *ACS Macro Lett.* **2019**, *8*, 500–505.
66 Wang, W. J.; Wang, W. P.; Wang, F.; Xie, X. F.; Yi, G.; Li, Z. B. Tough and body-temperature self-healing polysiloxane elastomers through building a double physical crosslinking network *via* competing non-covalent interactions. *J. Mater. Chem. A* **2022**, *10*, 23375–23383.
67 Du, R. C.; Xu, Z. C.; Zhu, C.; Jiang, Y. W.; Yan, H. P.; Wu, H.C.; Vardoulis, O.; Cai, Y. F.; Zhu, X. Y.; Bao, Z. N.; Zhang, Q. H.; Jia, X. D. A highly stretchable and self-healing supramolecular elastomer based on sliding crosslinks and hydrogen bonds. *Adv. Funct. Mater.* **2020**, *30*, 1907139.
68 Lai, J.; Jia, X. Y.; Wang, D. P.; Deng, Y. B.; Zheng, P.; Li, C. H.; Zuo, J. L.; Bao, Z. N. Thermodynamically stable whilst kinetically labile coordination bonds lead to strong and tough self-healing polymers. *Nat. Commun.* **2019**, *10*, 1164.
69 Yuan, T.; Cui, X. M.; Liu, X. K.; Qu, X. X.; Sun, J. Q. Highly tough, stretchable, self-healing, and recyclable hydrogels reinforced by *in situ*-formed polyelectrolyte complex nanoparticles. *Macromolecules* **2019**, *52*, 3141–3149.
70 Fang, X.; Li, Y. X.; Li, X.; Liu, W. M.; Yu, X. H.; Yan, F.; Sun, J. Q. Dynamic hydrophobic domains enable the fabrication of mechanically robust and highly elastic poly(vinyl alcohol)-based hydrogels with excellent self-healing ability. *ACS Mater. Lett.* **2020**, *2*, 764–770.
71 Wu, D. L.; Liu, L.; Ma, Q. H.; Dong, Q.; Han, Y. Q.; Liu, L.; Zhao, S. F.; Zhang, R. L.; Wang, M. J. Biomimetic supramolecular polyurethane with sliding polyrotaxane and disulfide bonds for strain sensors with wide sensing range and self-healing capability. *J. Colloid Interface Sci.* **2023**, *630*, 909–920.
72 Wang, L. P.; Zhang, M. G.; Hao, J. C.; Wang, X. Insertion of supramolecular segments into covalently crosslinked polyurethane networks towards the fabrication of recyclable elastomers. *Chinese J. Polym. Sci.* **2022**, *40*, 321–330.
73 Kim, S. M.; Jeon, H.; Shin, S. H.; Park, S. A.; Jegal, J.; Hwang, S. Y.; Oh, D. X.; Park, J. Superior toughness and fast self-healing at room temperature engineered by transparent elastomers. *Adv. Mater.* **2018**, *30*, 1705145.

https://doi.org/10.1007/s10118-023-2992-5